JOURNAL OF AEROSOL MEDICINE AND PULMONARY DRUG DELIVERY
Volume 27, Number 5, 2014
© Mary Ann Liebert, Inc.
Pp. 371–385
DOI: 10.1089/jamp.2013.1077

Optimal Delivery of Aerosols to Infants During Mechanical Ventilation

P. Worth Longest, PhD,[1,2] Mandana Azimi, MPharm,[2] and Michael Hindle, PhD[2]

Abstract

Purpose: The objective of this study was to determine optimal aerosol delivery conditions for a full-term (3.6 kg) infant receiving invasive mechanical ventilation by evaluating the effects of aerosol particle size, a new wye connector, and timing of aerosol delivery.
Methods: *In vitro* experiments used a vibrating mesh nebulizer and evaluated drug deposition fraction and emitted dose through ventilation circuits containing either a commercial (CM) or new streamlined (SL) wye connector and 3-mm endotracheal tube (ETT) for aerosols with mass median aerodynamic diameters of 880 nm, 1.78 μm, and 4.9 μm. The aerosol was released into the circuit either over the full inhalation cycle (T1 delivery) or over the first half of inhalation (T2 delivery). Validated computational fluid dynamics (CFD) simulations and whole-lung model predictions were used to assess lung deposition and exhaled dose during cyclic ventilation.
Results: *In vitro* experiments at a steady-state tracheal flow rate of 5 L/min resulted in 80–90% transmission of the 880-nm and 1.78-μm aerosols from the ETT. Based on CFD simulations with cyclic ventilation, the SL wye design reduced depositional losses in the wye by a factor of approximately 2–4 and improved lung delivery efficiencies by a factor of approximately 2 compared with the CM device. Delivery of the aerosol over the first half of the inspiratory cycle (T2) reduced exhaled dose from the ventilation circuit by a factor of 4 compared with T1 delivery. Optimal lung deposition was achieved with the SL wye connector and T2 delivery, resulting in 45% and 60% lung deposition for optimal polydisperse ($\sim$1.78 μm) and monodisperse ($\sim$2.5 μm) particle sizes, respectively.
Conclusions: Optimization of selected factors and use of a new SL wye connector can substantially increase the lung delivery efficiency of medical aerosols to infants from current values of $<$1–10% to a range of 45–60%.

Key words: respiratory drug delivery, mechanical ventilation, neonate, aerosols, streamlined wye, nebulization, CFD simulations, Monte Carlo modeling

Introduction

In adult patients receiving mechanical ventilation, a number of current and newly proposed aerosolized medications have demonstrated measurable benefits.[1,2] However, the use of inhaled pharmaceutical aerosols with neonates and infants receiving mechanical ventilation has yielded mixed outcomes. Some clinical studies of respiratory drug delivery in ventilated infants have demonstrated reduced need for systemic glucocorticoids,[3] improved oxygenation,[4] and increased fluid resorption.[5] In contrast, other studies of inhaled pharmaceutical aerosols in infants have demonstrated no measurable benefits.[6,7] It is currently hypothesized that low lung delivery efficiencies, poorly controlled dosing, and high dose variability are partly responsible for these inconsistent and mixed clinical results.[8,9]

The delivery efficiency of pharmaceutical aerosols to the lungs of infants is known to be low and highly variable.[8–10] Aerosol drug depositional loss occurs in the aerosol generator, interface device, and ventilation circuit including the endotracheal tube (ETT), which has an internal diameter (ID) of approximately 3 mm in ventilated newborn infants. Additional challenges to lung deposition of pharmaceutical aerosols in infants include low tidal volumes, short inhalation periods, which increase inertial effects, high breathing frequencies, and small inspiratory:expiratory (I:E) ratios.[8,10]

[1]Department of Mechanical and Nuclear Engineering, Virginia Commonwealth University, Richmond, VA.
[2]Department of Pharmaceutics, Virginia Commonwealth University, Richmond, VA.

With conventional jet nebulizers and metered dose inhalers (MDIs), delivery efficiency to the lungs of intubated infants is typically 1% and below.[11–14] This extremely low delivery efficiency has been consistently demonstrated based on *in vitro* experiments[13,14] and animal models,[11,13,15] and in humans.[16] Newer vibrating mesh and ultrasonic nebulizers have significantly increased lung delivery efficiency of aerosols for ventilated infants to a value of approximately 10% in some cases.[11,17,18] For example, in a macaque animal model of infant mechanical ventilation with a 3-mm ETT, continuous and inhalation synchronized mesh nebulizers resulted in 12.6% and 14% lung delivered doses, respectively.[11]

New aerosol generation technologies, like vibrating mesh nebulizers, provide a clear improvement in dose delivery to infants on mechanical ventilation. However, the cost of these devices is significantly more than that of jet-based technologies, and frequent cleaning is required. Even with recent improvements in delivery efficiency,[11,18] waste of the aerosolized medication remains high with 6–9 times more drug lost in the ventilation circuit than delivered to the lungs. These high losses may limit the use of expensive medications as an aerosol and increase delivery time. Furthermore, dose variability is high for all systems used to deliver aerosols to infants.[8,16] For example, animal models with all nebulizer types result in 0.05% to approximately 15% delivery efficiency, representing a 2–3 order of magnitude difference in lung dose.[8,11] High depositional losses in the ventilation circuit can dramatically change the lung delivered dose if the system is modified by a small amount, *e.g.*, use of a 3.5- vs. 3.0-mm ID ETT. Finally, it is not clear where aerosolized medicines are delivered within the airways of ventilated infants. From *in vivo* studies, Fok *et al*.[16] reported a high fraction of the delivered 1% dose resides in the central airways. Using an MDI and rabbit model, Everard *et al*.[13] demonstrated three- to fivefold more dose in the trachea and main bronchi than in the remainder of the lungs. Effective aerosol therapy requires that the medication be delivered to its intended site of action within the airways at a controlled dose.

Aerosol size is known to have a significant effect on lung delivery efficiency. Deposition mechanisms in both the ventilation circuit and lung for typical medical aerosols are impaction, sedimentation, and turbulent dispersion, all of which are decreased by reducing the aerosol particle or droplet size. Depositional losses in the ventilation circuit can therefore obviously be reduced by using a smaller aerosol. For example, Ahrens *et al*.[19] implemented an *in vitro* model of aerosol delivery during mechanical ventilation with a range of ETT sizes and demonstrated that lung delivery efficiency could be increased 9 times by using an aerosol with a mass median aerodynamic diameter (MMAD) of 0.54 μm compared with a conventional size of approximately 4 μm. The limit to the minimum aerosol size that can be used for effective lung delivery is the need to have particles with sufficient mass for lung deposition. *In vitro* models often neglect the exhaled drug fraction and assume that the dose exiting the ETT is deposited in the lungs. However, particles smaller than approximately 2 μm are often exhaled at a high fraction in adults.[20–22] Previous whole-lung simulations of aerosol deposition in children indicate that, for typical micrometer particles, infants have higher lung deposition fractions (DFs) than adults.[23–25] However, this is a complex problem involving both dimensions of the airways and inspiration rates along with multiple aerosol deposition mechanisms. Selection of an optimal particle size for drug delivery to infants receiving mechanical ventilation should seek to both minimize ventilation circuit losses and maximize deposition and retention in the lungs.

Sites of high aerosol depositional losses in the ventilation circuit are typically the wye connector and ETT. The size of the ETT is limited by the patient's anatomy; however, larger tubes are known to transmit more aerosol.[13,19] Few studies have attempted to modify the wye geometry for improved aerosol delivery. Ivri and Fink[26] proposed low angles ($<15°$) in ventilation circuit components to minimize depositional losses. However, this approach may not be practical for modifying the wye connector where a 90° change in flow direction is required. In a recent study by Mazela *et al*.,[12] a redesigned wye, referred to as the VC connector, was shown to increase emitted dose (ED) in a premature neonate *in vitro* model. As an alternative approach, Longest *et al*.[27] recently described streamlined (SL) designs of mechanical ventilation components to minimize aerosol losses. In this approach, sudden changes in flow direction and cross-sectional area are replaced with components that include gradual changes and a minimum radius of curvature. Longest *et al*. demonstrated that a SL design reduced depositional loss in the T-connector for a mesh nebulizer from approximately 30% to 5% during adult noninvasive ventilation.[27]

The timing of aerosol release or delivery into the ventilation circuit along with positioning of the generation device may have an effect on lung delivery efficiency in ventilated infants. Synchronizing aerosol delivery with inhalation is known to reduce exhalation losses in adults.[28] However, synchronization has resulted in varying delivery outcomes for infants. Turpeinen and Nikander[29] demonstrated improved lung delivery using synchronization in an *in vitro* model of neonatal ventilation with the nebulizer positioned below the wye connector. However, this configuration may increase ventilator dead space and the rebreathing of expired CO_2 during the ventilation process. Other studies with mesh nebulizers have indicated that synchronization had no significant effect on delivery[11] or a negative effect on aerosol delivery efficiency.[17] Given the low tidal volumes delivered during infant ventilation, positioning of the aerosol source also determines the amount of aerosol entering the lungs during inhalation. However, a recent study by Ari *et al*.[18] showed a nebulizer position effect only in adults and not in a pediatric *in vitro* model of aerosol delivery.

As described, appropriate selection of nebulizer type, aerosol particle size characteristics, circuit components, and delivery timing may all have an impact on lung delivery and deposition of aerosols in ventilated patients. Currently, the best performing systems implement a mesh nebulizer and can achieve approximately 10% delivery efficiency to infant lung models.[11,17] However, a systematic evaluation of multiple relevant factors may further increase the lung deposition efficiency and reduce variability of aerosols administered to ventilated infants. Furthermore, the distribution of deposited drug within the lungs of ventilated infants is currently not known. Considering the low tidal volumes associated with infant ventilation in conjunction with previous findings,[13,16] aerosol may not reach the alveolar airspace.

The objective of this study is to determine optimal aerosol delivery conditions for an infant receiving invasive mechanical ventilation by evaluating the effects of a new wye connector, aerosol particle size, and timing of aerosol delivery. A full-term infant is considered with a tidal volume of approximately 25 mL, inspiratory time of 0.3 sec, and a 3-mm ID ETT. Aerosol delivery efficiency of a commercial (CM) wye is compared with a new SL design. Methods include a combination of *in vitro* experiments, computational fluid dynamics (CFD), and whole-lung deposition modeling. The strengths of each method are leveraged to determine optimal delivery and lung deposition conditions, including the effect of aerosol exhalation. The *in vitro* experiments are first implemented to evaluate effects of the SL wye designs over a range of aerosol particle sizes and to validate the CFD model. The CFD simulations evaluate the effects of cyclic ventilation waveforms and aerosol delivery timing across a range of particle sizes. Results of the CFD model are then used as input for a whole-lung Monte Carlo model that predicts deposition throughout the lung airways as well as the exhaled fraction. Both particle size and delivery timing are considered in order to determine optimal conditions that maximize lung aerosol deposition, minimize aerosol exhalation, and deliver a high fraction of the aerosol to specific lung regions.

Materials and Methods

Aerosol generation and ventilation circuit components

Aerosols were generated using a vibrating mesh nebulizer based on the improved performance of this approach compared with other aerosol sources in previous studies.[11,18] The Aeroneb Lab mesh nebulizer (Aerogen Limited, Galway, Ireland) was implemented in all cases; it was previously characterized and shown to produce a smaller aerosol than the typically implemented Aeroneb Pro device.[30] A range of realistic aerosol particle sizes was then generated by connecting the nebulizer with either a custom mixer-heater device or a CM neonatal T-connector (Aerogen Limited). The mixer-heater was previously developed and optimized by Longest *et al.*[31] to modify aerosol particle size with controlled heat and humidity conditions along with low (<10%) depositional loss of the drug. As described by Longest *et al.*,[31] the mixer-heater operates with air flow rates in the range of 5–30 L/min and aerosol nebulization rates of approximately 0.2–0.4 mL/min, but can be extended to other flow rates by adjusting the heating controls. Based on theoretical calculation, albuterol sulfate (AS) concentrations in the nebulizer solution were selected as 0.2% and 5% w/v to produce approximate aerosol particle sizes exiting the mixer-heater of 900 nm and 2 μm, respectively. The Aeroneb Lab nebulizer was also used in the neonatal T-connector, which has a 10-mm outlet, to provide a larger and more conventional aerosol particle size of approximately 4–5 μm. For the small and intermediate aerosol particle sizes generated with the mixer-heater, the aerosol exited the device in a heated airstream that was humidified through droplet evaporation.[31] For the larger aerosol generated in the neonatal T-connector, humid air [>90% relative humidity (RH)] was supplied to the device at a temperature of 25°C from a Vapotherm 2000i unit (Vapotherm Inc., Stevensville, MD). For both the mixer-heater and neonatal T-connector aerosol generation setups, a 10-cm length of infant ventilator tubing (ID of 10 mm) served to transport the aerosol to the wye connectors.

CM and SL wyes were compared to determine their aerosol delivery efficiencies. The CM device was included in a neonatal conventional ventilation circuit (Teleflex Medical, Research Triangle Park, NC) with connections for inspiratory and expiratory 10-mm lines, which form a 60° angle with each other (Fig. 1a). The 10-cm inlet tubing and start of the wye connector are marked in the figure. To improve aerosol delivery, a new SL wye was constructed based on the approach of Longest *et al*. and preliminary CFD simulations (Fig. 1b).[27] In the SL design, sharp changes in flow direction were replaced with more gradual changes. The centerline radius of curvature between the inspiratory/expiratory lines and ETT was approximately 1 cm. The ETT was aligned with the end of the junction region opposite the inspiratory/expiratory lines (Fig. 1b), which is important to avoid further changing the direction of the high-speed flow as it enters the ETT. Sigmoidal curves were then used to connect the wye junction region with the ETT (Fig. 1b). Specifically, the junction is designed such that fluid moving along the outside of the wye connector experiences a smooth 90° bend. The mismatch in diameters between the inspiratory/expiratory lines and ETT is accommodated using a sigmoidal curve in which the ends of the curve are tangent to each other. Radii of curvatures describing the two ends of the sigmoidal curve in the midplane of the geometry are approximately 1 cm. The resulting SL geometry does not increase the overlapping inspiratory–expiratory volume or the dead space of the

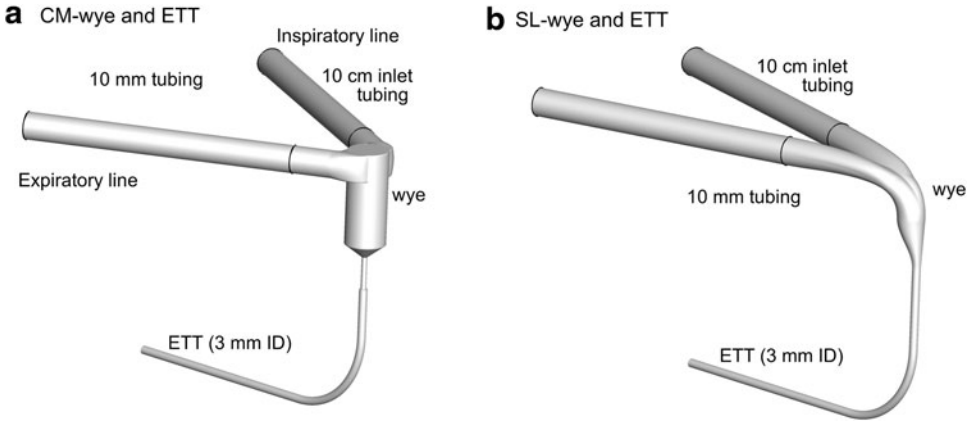

FIG. 1. Invasive mechanical ventilation circuits for neonates with 10-mm inspiratory and expiratory tubing, the **(a)** commercial (CM) and **(b)** streamlined (SL) wye connectors, and an endotracheal tube (ETT) with a 3-mm internal diameter. The division between the 10-mm diameter inlet tubing and wye connectors is marked with a dark line.

ventilation circuit. Preliminary CFD simulations demonstrated a low level of flow separation and disruption during both inspiration and expiration with the SL design. Both wye geometries were connected to an ETT with a 3-mm ID (PedSoft, Hudson RCI/Teleflex Medical) and uncut length of 146 mm. The ETT was curved through a 90° bend to represent passage through the oropharyngeal region. The centerline radius of curvature for the ETT bend was 30 mm, and the straight section downstream of the bend had a length of 78 mm.

Infant lung model and ventilation parameters

The airway model was based on a full-term newborn infant with an average weight and height of 3.6 kg and 50 cm, respectively, based on the Centers for Disease Control and Prevention growth chart.[32] Dimensions of the tracheobronchial (TB) airways were determined from the study of Phalen *et al.*,[23] which provides correlations for pediatric airway lengths and diameters based on subject height. The Phalen *et al.*[23] dataset was developed from infant airway cast measurements with ages ranging from 0.03 to 21 years. The alveolar model was based on the study of Hofmann *et al.*,[24] who used anatomical data from Dunnill.[33] Due to a mismatch in the two datasets, the alveolar model was scaled in length and diameter so that the inlet of airway bifurcation 16 (B16; start of the alveolar region) matched the outlet of B15 (end of the TB region). Infants have fewer alveolar bifurcations than adults, and the final alveolar sacs were assumed to occur approximately at the outlet of B20.[24] The alveolar sacs had a diameter of 0.26 mm available for flow and were not assumed to move with respiration in this study. Total airway volume was 68 cm^3 with the total TB volume (through B15) equal to 16.7 cm^3.

Ventilation characteristics of the 3.6-kg newborn infant were based on the recommendations of Walsh and DiBlasi.[34] Time-based parameters were a frequency of 40 breaths/min, period of 1.5 sec, and inspiratory time of 0.3 sec. Tidal volume per weight was set to 7 mL/kg, resulting in an inhaled volume of approximately 25 mL. The transient flow rate was approximated with a sine wave pattern having maximum inspiratory and expiratory flows of 7.8 and 2.0 L/min, respectively. Bias flow and a breath pause were not included. The resulting minute ventilation (breathing frequency times tidal volume) and mean tracheal inspiratory flow were 1 L/min and 5 L/min, respectively.

It is expected that timing of the aerosol delivery may improve delivery efficiency in mechanically ventilated infants. However, aerosol delivery over a portion of the inspiratory waveform has not previously been considered during mechanical ventilation. In this study, two aerosol injection strategies were considered. In the first delivery approach (T1), the aerosol delivery was synchronized with inhalation and occurred over the full inhalation cycle. The second strategy (T2) only injected the aerosol over the first half (0.15 sec) of the inhalation phase. The T2 approach is expected to transport a higher fraction of the aerosol deeper into the airways and minimize exhalation of the particles.

In vitro *experiments*

In vitro experiments were conducted to evaluate initial aerosol particle sizes and deposition within the CM and SL wye systems, including a 3-mm ETT, at a steady-state flow rate of 5 L/min. This flow rate is consistent with the tracheal inspiratory flow rate of a ventilated newborn infant as described in the previous section. To form the three target aerosol sizes, the drug formulation was aqueous-based with AS concentrations in deionized water of 0.2% w/v (small aerosol and mixer-heater), 5% (intermediate aerosol and mixer-heater), and 0.2% (large aerosol and neonatal T-connector). The Aeroneb Lab nebulizer was operated for 2 min for the small and intermediate experiments, resulting in mean [standard deviation (SD)] nominal doses of approximately 308 (56) μg and 2,357 (183) μg, respectively. For the large aerosol, the nebulizer was operated for 30 sec with a mean (SD) nominal dose of 604 (161) μg. These nominal doses are the drug mass that was delivered to the 10-cm inlet tubing leading to the CM or SL wye connectors (Fig. 1).

To determine the aerodynamic droplet size distribution exiting the mixer-heater and exiting the Aeroneb Lab nebulizer, an Andersen Cascade Impactor (ACI; Graseby-Andersen Inc., Smyrna, GA) was used operating at 30 L/min and housed in an environmental cabinet (Espec, Hudsonville, MI). For the aerosols that were generated from the mixer-heater, aerosol flow rates of 30 L/min for the 0.2% AS formulation and 5 L/min for the 5% formulation, respectively, were used. These aerosols were sampled via 50 cm × 10 mm diameter ventilator tubing positioned with a gap of 10 mm to the inlet of the ACI. Decreasing the aerosol flow rate entering the impactor allows a higher fraction of entrained air to enter the ACI from the cabinet, which may affect the measured particle size distribution. However, during each particle sizing experiment, no changes in the cabinet temperature were observed and the humidity remained above 90% RH. The temperature of the aerosol exiting the ventilator tubing was 37°C. In order to minimize evaporative or condensation size changes of the aerosols exiting the mixer-heater, the aerosols were sized with the impactor held at isothermal conditions compared with the aerosol. The impactor was equilibrated in the environmental cabinet for at least 20 min prior to sizing. The mixer-heater–generated aerosols were then sampled into the ACI held at 37°C. The humidity of the environmental cabinet was >90% RH in order to minimize size change of the aerosols arising from unwanted evaporation and condensation during measurement.

The aerosols that were generated from the Aeroneb Lab nebulizer were sampled directly into the ACI. A gap distance of approximately 10 mm separated the Aeroneb outlet and the ACI inlet, allowing for the entrainment of humidified air at a rate of 30 L/min. The nebulizer and impactor, as well as the ACI, were placed in the environmental cabinet (Espec) and equilibrated at 25°C for at least 20 min, ensuring isothermal conditions during sizing. The humidity of the environmental cabinet was >90% RH in order to again minimize size change of the aerosols arising from unwanted evaporation and condensation during measurement.

Drug deposition on the ACI collection plates for the initial size experiments was determined following washings using appropriate volumes of deionized water (10–20 mL). The solutions were then assayed using a validated high-performance liquid chromatography–ultraviolet (HPLC-UV) method for AS. The mass of AS on each impaction plate was determined and used to calculate the

aerodynamic particle size distribution of the drug. The MMAD was defined as the particle size at the 50th percentile on a cumulative percent mass undersize distribution (D50) using linear interpolation. The mass of formulation nebulized was determined by weighing the nebulizer before and after each experiment. The solution AS concentration and the mass of formulation nebulized were used to determine the nominal dose of AS delivered.

To determine aerosol deposition in the SL wye, a rapid prototyping process was used to create a physical model of the wye. The wye design that was developed from preliminary CFD simulations was given a wall thickness of approximately 1 mm in a solid modeling program. A Viper SLA system (3D Systems, Valencia, CA) was used to construct the SL wye design using Accura 60 clear plastic resin. The resolution of the prototyper was 0.1 mm, and the final surface finish of the SL components was smooth.

In vitro experiments were conducted to determine aerosol drug deposition within individual components of the delivery system, as well as ED exiting the ETT at a steady-state flow rate of 5 L/min. The mixer-heater was operated at 30 L/min to provide an aerosol that was consistent with the sizing experiments. This aerosol stream was split using an SL connector with 25 L/min directed to a waste filter and 5 L/min flowing to the inspiratory arm of the wye connector. For the neonatal T-connector aerosol, a Vapotherm 2000i (Vapotherm Inc.) humidification unit was implemented to supply steady-state airflow with RH of >90% and temperature of 25°C at a flow rate of 5 LPM. The *in vitro* models were tested under ambient room conditions (23–25°C). One limitation of this approach is that the aerosol exiting the mixer-heater at 37°C may cool during passage through the experimental setup, which may lead to condensational growth of the aerosol as the temperature decreases during passage through the tubing. However, such cooling is expected to be minimal due to the short flow paths and relatively high velocities encountered by the aerosol prior to deposition on the final filter. This effect was avoided by using 25°C air in the neonatal T-connector, which produced an approximate thermally neutral system and prevented condensation of the high-humidity airflow. In the experiments, the expiratory side of the wye connector was closed to allow for only inspiratory airflow. The dose emitted from the ETT was captured on a high-efficiency filter (Pulmoguard II, Quest Medical, Brockton, MA).

Drug deposition in the nebulizer, individual system components, and on the outlet filter was determined with a validated HPLC-UV assay method. As with the particle sizing experiments, the mass of nebulized formulation was determined by weighing the nebulizers. Drug deposition in the Aeroneb Lab device was below 5%. Drug deposition and ED were calculated as percentages of the drug mass leaving the mixer-heater for the small and intermediate aerosols (900 nm and 2 μm) and the mass leaving the nebulizer for the conventional aerosol particle size (4–5 μm). At least four replications of each experiment were performed.

CFD simulations

CFD simulations were performed to validate the model under steady-state conditions, evaluate deposition and ED during cyclic breathing, and provide input conditions for the whole-lung Monte Carlo model. Isothermal, incompressible, and constant-property flow was assumed in all cases. For an inlet flow rate of 5 L/min, the Reynolds numbers in the 10-mm inlet tubing and 3-mm ETT were 689 and 2,300, respectively, which indicates laminar through turbulent flow conditions in the complex ventilation circuit geometry.

The flow fields in the wye geometries were solved using Fluent 12 (Ansys Inc., Canonsburg, PA) with a steady or transient solution and the low Reynolds number (LRN) κ-ω two-equation turbulence model. This turbulence model was selected based on a combination of its accuracy and high efficiency, compared with more complex methods, such as large eddy simulation. Considering aerosol transport, the LRN κ-ω model was previously shown to accurately predict particle transport and deposition for both monodisperse and polydisperse aerosol distributions in airway models and delivery devices on a regional and highly localized basis.[35–38]

Computational grids of the airflow passages were constructed based on previously established best practices.[39,40] The resulting meshes representing the wye connectors with ETTs for the CM and SL designs contained approximately 774,000 and 829,000 cells, respectively. Grid convergence of these meshes was established by comparing with meshes containing at least 30% fewer cells in each case. These comparisons indicated that there were minimal differences (< 5% relative error) in the maximum velocity and particle deposition values between the grids initially established in this study and the ones with 30% fewer cells. As a result, the finer meshes (more cells) were considered sufficient and used in all subsequent simulations.

Droplet trajectories and deposition were determined in the CM and SL wye connectors using a previously developed Lagrangian tracking algorithm.[41,42] Factors affecting particle motion included in the transport equations were drag, gravity, and turbulent dispersion. Previously developed near-wall corrections for interpolating velocity and directionally-dependent turbulence were included.[41,43] Due to the use of humidified airflow in the experiments, droplet evaporation was not included in the model, resulting in the simulation of particle trajectories with unchanging diameters. Specifically, AS particles, when inhaled with environmental air, are known to increase in size due to the drug being mildly hygroscopic.[44–46] However, the RHs exiting both the mixer-heater and Aeroneb nebulizer were high such that additional size change of the particles was not expected to be significant. The overall MMAD of the polydisperse aerosol changes as the polydisperse particles move through the system and are selectively filtered by deposition.

CFD simulations of deposition are based on both the polydisperse particle distributions measured in the experiments and monodisperse individual particle sizes. The polydisperse size distributions are used to validate the CFD predictions and to provide a realistic approximation of delivery efficiency that can be achieved with current mesh nebulizers. However, aerosols produced by most current mesh nebulizers in a humidified airstream are known to be bimodal, such that the larger size in the distribution limits delivery efficiency through the wye and ETT. To determine optimal particle size conditions for aerosol transmission through the wye system, monodisperse aerosols with

individual sizes ranging from 200 nm to 10 μm were also considered. CFD predictions of DF are based on initial drug mass of the polydisperse or monodisperse aerosol entering the geometry, unless otherwise noted. To resolve the polydisperse aerosol distribution, 27,000 representative particles were simulated with 3,000 particles used to resolve nine discrete size fractions selected as the midpoint diameters of the ACI stages. Simulation of monodisperse particle sizes implemented 3,000 particles. It was determined that increasing the number of representative polydisperse and monodisperse particles had a negligible effect on the predicted particle DFs. Particles were initialized over the circular cross-section of the 10-mm inlet tubing using a parabolic inlet profile, as described by Longest and Vinchurkar.[37]

Whole-lung Monte Carlo model

To simulate aerosol transport and deposition through the infant airway geometry, a whole-lung Monte Carlo model was implemented, similar to the approach described by Koblinger and Hofmann.[47,48] Either a monodisperse aerosol or the polydisperse distributions predicted by CFD simulations exiting the ETT were initialized in the trachea. The release time of the aerosol was based on CFD predictions of the time distribution that the particles exited the ETT. Cyclic breathing was simulated consistent with the infant inspiratory profile described previously, which has a 0.3-sec inhalation and 1.2-sec exhalation period. Mean inspiratory and expiratory flow rates were 5 and 1.24 L/min, respectively. In the Monte Carlo approach,[47,49] a randomly generated path through the lung airways is defined. Branch diameters, lengths, and bifurcation angles are statistically determined based on mean values and SDs using a random-number generator and assuming a normal distribution. Transport and deposition through this path is simulated based on deposition correlations for impaction, sedimentation, and diffusion. Additional random pathways are then simulated until deposition within each lung region and bifurcation converges within a specified range. Simulations for 50,000 particles with 1,000 particles per path were conducted, and doubling this number of particles and paths had a negligible impact on deposition predictions. Although model predictions provide branch-averaged deposition results, regional deposition is reported with B1–B15 defining the TB region and B16–B20 representing the alveolar airways. Previous comparisons of model results with the *in vivo* fast-clearance and slow-clearance data of Heyder *et al*.[20] for adults showed very good agreement.

Results

In vitro *measurements of particle size distributions*

Polydisperse size distributions for the three target sizes based on cascade impaction measurements are reported in Figure 2 in terms of mass fraction per micrometer and midpoint sizes of the ACI stages. Measured MMADs (and SDs) for the small, intermediate, and conventional aerosol particle sizes were 880 (20) nm, 1.78 (0.07) μm, and 4.90 (0.3) μm, respectively. These values are very close to the target sizes, indicating that solution concentration can be used to control aerosol particle size exiting the mixer-heater. The 4.9-μm aerosol (produced with the neonatal T-connector) is observed to be bimodal with 30% of the aerosol mass in the larger size mass fraction above 6 μm. In contrast, use of the mixer-heater produces monomodal small and intermediate aerosols with geometric standard deviations (GSDs) of 1.9 and 1.7, respectively.

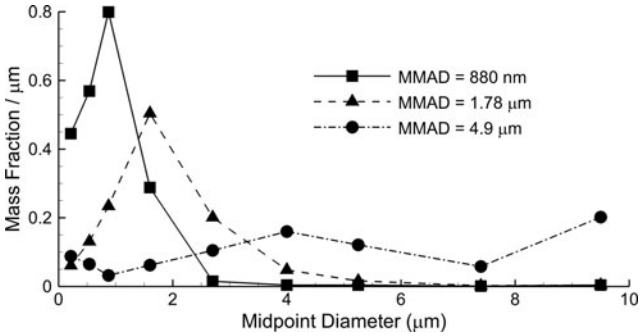

FIG. 2. Initial polydisperse size distribution of the aerosol in terms of mass fraction per micrometer (bin size) based on measurements with the ACI (~30 L/min) at the inlet of the delivery system.

In vitro *measurement of drug deposition*

DFs in individual system components are presented in Table 1 from *in vitro* measurements at the tracheal inlet flow rate of 5 L/min. The inlet DF is determined in the 10-cm tubing length leading from the mixer-heater or neonatal T-connector to the wye geometry. DF in the device is the sum of values in individual components and includes the additional fraction deposited in the neonatal T-connector used for the conventional 4.9-μm aerosol. Values of DF_{filter} represent the ED from the ETT entering the lungs. For the CM wye, aerosol particle size (880 nm and 1.78 μm) was shown to significantly ($p < 0.05$; t test) reduce DF in all components compared with the conventional 4.9-μm diameter aerosol (Table 1). Values of DF in the CM wye and ETT decrease by a factor of 3–20 as MMAD decreases from 4.9 μm to 880 nm. As a result, the filter DF (ED) is 12.3% for the 4.9-μm aerosol and increases to 87.6% for the 880-nm aerosol. With the SL wye, there was no significant change in device DF between the 880-nm and 1.78-μm aerosols ($p = 0.112$; t test). For these small and intermediate aerosol particle sizes and the SL geometry, total DF is approximately 10%, with DF_{filter} equal to approximately 90%. Considering the 1.78-μm aerosol, the SL wye system reduces total device deposition by a factor of 2 compared with the CM system.

CFD predictions of flow-field characteristics

CFD predictions of the velocity field and turbulent viscosity ratio are presented in Figures 3 and 4, respectively, at a steady-state inspiratory flow of 5 L/min. Considering the velocity field, the CM wye geometry displays a high degree of vortical mixing and flow disruption in the junction region and a high-velocity jet entering the ETT. Strong turbulent dissipation reduces the maximum velocity in the ETT of the CM wye geometry. In contrast, the SL wye provides a smooth transition between the inlet and ETT with reduced flow disruption and recirculation. With the SL design, higher velocities are observed on the outside of the bend region, which could increase deposition by impaction. Velocity

Table 1. Deposition Fraction as a Percentage of Emitted Dose

Aerosols	DF_{inlet}	DF_{wye}	DF_{ETT}	DF_{device}[a]	DF_{filter}[b]
CM wye					
MMAD = 880 nm	3.1 (1.1)[d]	7.2 (3.5)[d]	2.1 (0.5)[d]	12.4 (4.2)[d]	87.6 (4.2)[d]
MMAD = 1.78 μm	2.9 (1.2)[d]	8.0 (4.5)[d]	9.3 (1.7)[d]	20.2 (5.0)[d]	79.8 (5.0)[d]
MMAD = 4.9 μm	5.6 (1.75)	25.6 (0.9)	40.7 (2.1)	87.7[c] (2.1)	12.3 (2.1)
SL wye					
MMAD = 880 nm	3.7 (1.7)	1.6 (1.0)[e]	1.9 (0.5)	7.2 (2.9)[e]	92.8 (2.9)[e]
MMAD = 1.78 μm	2.5 (1.4)	1.6 (0.9)[e]	6.7 (0.7)[e]	10.9 (2.2)[e]	89.1 (2.2)[e]

The table presents mean (SD) deposition fraction (DF) as a percentage of dose emitted from the mixer (880-nm and 1.78-μm aerosols) or nebulizer (4.9-μm aerosol) at a steady-state flow rate of 5 L/min for the commercial (CM) and streamlined (SL) cases based on *in vitro* experiments.

[a]Total device DF.

[b]Equal to the emitted dose (ED) from the ETT.

[c]Value includes a DF of 15.9% in the neonatal T-connector, which was not present in the other aerosol cases.

[d]Statistically significant difference in DF compared with the DF observed for the 4.9-μm MMAD aerosol ($p < 0.05$; t test).

[e]Statistically significant difference in DF for the SL setup compared with the DF observed for the same sized aerosol delivered through the CM setup ($p < 0.05$; t test).

fields for the CM and SL systems are similar in the region distal to the ETT bend, as expected.

Turbulent viscosity ratio is calculated as turbulent plus laminar viscosity divided by laminar viscosity and represents the effects of turbulence on the flow field. Prevalent values of this ratio near 10 indicate that turbulence has increased the effective viscosity of the flow field by 10-fold compared with laminar flow. As a result, turbulence has a strong influence on flow in both the CM wye and SL wye geometries. Elevated values of turbulent viscosity ratio throughout the ETTs indicate the potential for aerosol deposition from turbulent fluctuations (*i.e.*, dispersion).

CFD predictions of deposition with steady-state flow

CFD predictions of polydisperse aerosol DFs based on drug mass are compared with experimental results at a steady inlet flow of 5 L/min in Figure 5. Comparisons are made on the basis of individual components. To match experimental results of DF partitioning between the wye and ETT, the narrow 2-mm channel at the exit of the CM wye design was considered to be part of the ETT in the CFD simulations. This is reasonable considering that liquid droplets depositing in this region will likely flow into the ETT due to high shear. A similar correction was not needed for the SL model. In almost all cases, model predictions of DF are within the SD range of the experimental results. A few exceptions are observed in terms of wye and ETT partitioning of drug mass for the CM case. However, total device and ED results match very well between the predictions and experiments in all cases. As a result, model predictions are considered accurate for evaluating both steady-state and cyclic ventilation results. Furthermore, the agreement provides verification that experimental filter deposition is not the result of re-aerosolization of deposited liquid or liquid flowing along the surface of the ETT.

As with the *in vitro* data, the steady-state polydisperse CFD results illustrate a dramatic reduction in filter DF as the aerosol particle size is increased for the CM wye system. With the SL design, DFs in each component remain low (10%) for both the 880-nm and 1.78-μm aerosols, and filter DF is approximately 80–90% for these sizes. Results of the 4.9-μm aerosol in the SL geometry are evaluated for cyclic breathing based on CFD predictions in the next section.

Monodisperse aerosols can be used to investigate ideal particle sizes for delivery through the wye and ETT ventilation components. CFD predictions of DF in the wye and total device are presented in Figure 6 based on monodisperse

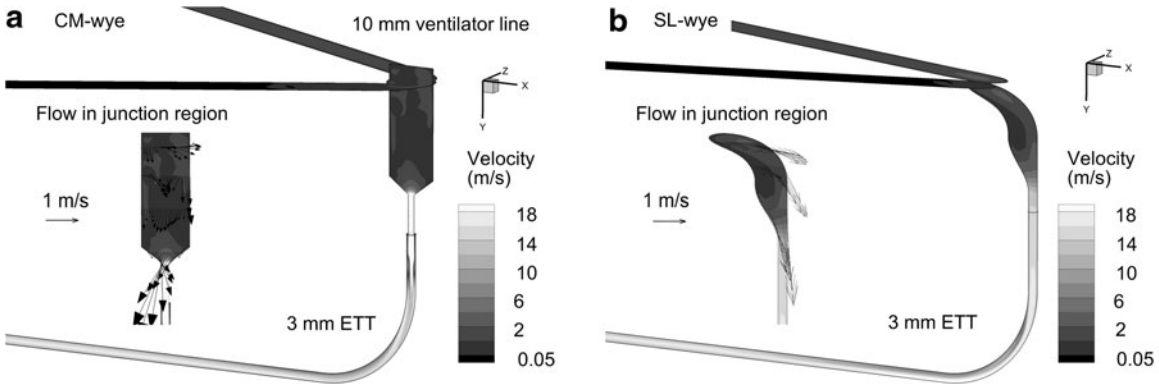

FIG. 3. Contours of velocity magnitude and velocity vectors on selected planes for the **(a)** CM wye and **(b)** SL wye systems at a steady-state inlet flow of 5 L/min.

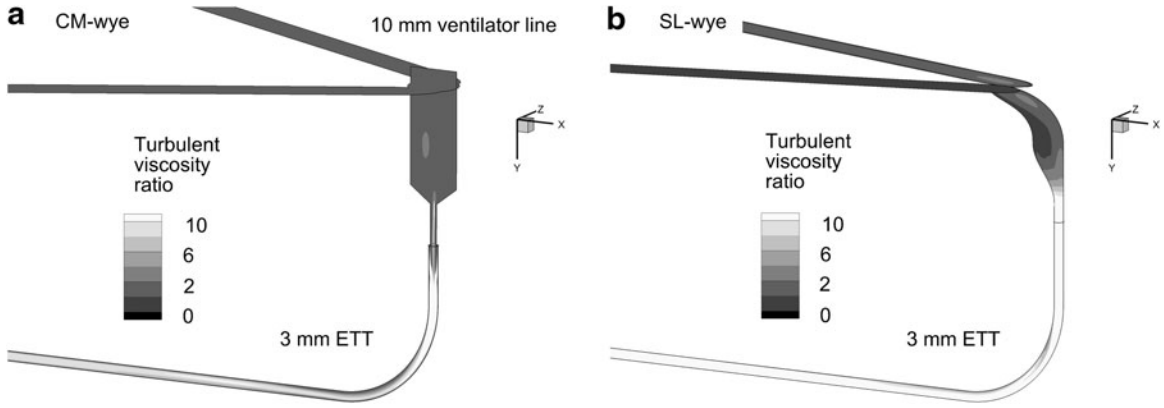

FIG. 4. Contours of turbulent viscosity ratio on selected planes for the **(a)** CM wye and **(b)** SL wye systems at a steady-state inlet flow of 5 L/min. The turbulent viscosity ratio represents the amount of viscosity increase occurring in the flow due to turbulent effects.

individual particle sizes and a steady-state inspiratory flow rate of 5 L/min. Considering deposition in the wye (Fig. 6a), a rapid rise in DF is observed with the CM device for aerosols greater than 4 μm. For the SL wye, depositional loss remains low and within a range of 10–20% for conventional-sized aerosols (4–7 μm). With a characteristic nebulizer particle size of 5.25 μm, DF in the wye geometry is reduced by a factor of sevenfold for the SL design (11.6%) versus the CM (68.2%). With the SL model, some of the additional transmitted dose is lost in the ETT. Therefore, it is important to consider the overall or total DF of the wye and ETT system. Figure 6b illustrates that the SL design reduces overall DF by a factor of approximately 2 in the range of 2–6-μm particles. Below 2 μm, total DF from both devices with monodisperse aerosols is less than 20%.

CFD predictions of deposition with cyclic ventilation

Cyclic ventilation using a transient inspiratory and expiratory sinusoidal waveform was simulated with the CFD model to capture both deposition and the aerosol fraction lost to the expiratory line (circuit exhaled dose). Particles were initialized at the inlet to the wye geometry and were delivered during either the full inspiration time (T1) or the first half of inspiration (T2). Considering deposition in the inlet and wye, cyclic results with T1 injection typically doubled DF for the smaller two aerosol particle sizes (Table 2) compared with the steady state (Table 1). Inlet-plus-wye deposition of the 4.9-μm aerosol is similar between the steady-state and transient simulations with the CM setup. In the ETT, steady-state versus T1 deposition results are

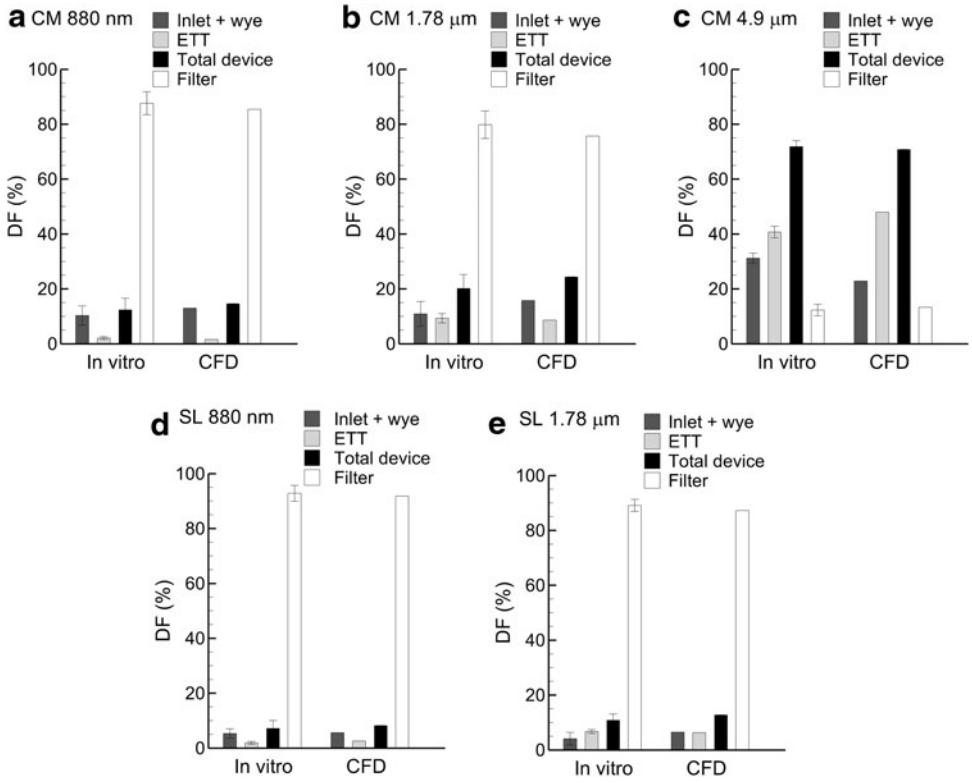

FIG. 5. *In vitro* measurements of DF compared with CFD results at a steady-state inspiratory flow of 5 L/min for the device and inlet particle (MMAD) size combinations of **(a)** CM and 880 nm, **(b)** CM and 1.78 μm, **(c)** CM and 4.9 μm, **(d)** SL and 880 nm, and **(e)** SL and 1.78 μm. Error bars on the *in vitro* results represent ± 1 SD.

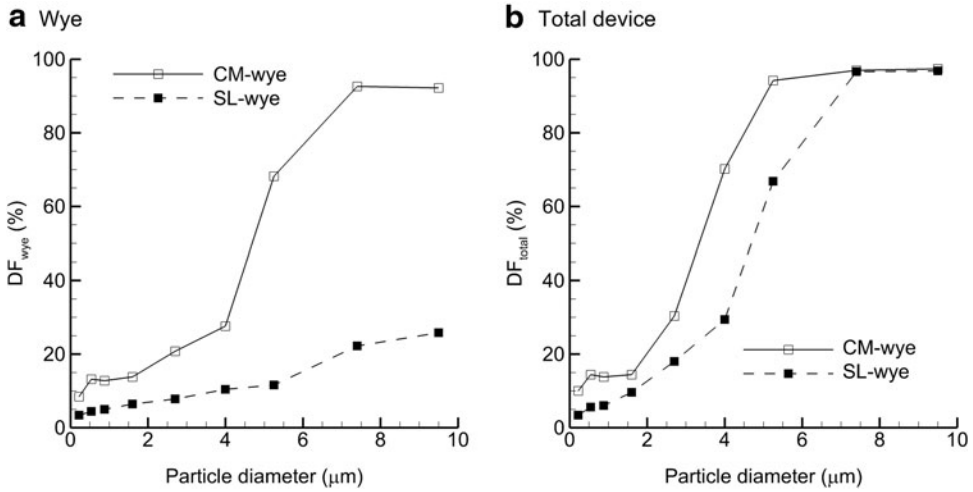

FIG. 6. DF of monodisperse particles across a range of particle sizes based on CFD simulations in the **(a)** wye-connector and **(b)** total device. Comparisons of CM and SL wye results demonstrate dramatic improvements in delivery efficiency.

very similar for all aerosol particle sizes considered and with both the CM and SL cases. ED for both the CM and SL setups with cyclic inhalation is largely reduced from steady-state predictions due to the circuit exhaled dose, especially for T1 conditions. With T1 delivery, circuit exhaled dose is approximately 30–40% of the AS drug mass entering the system for all sizes. Implementing the T2 delivery strategy, the circuit exhaled dose decreases by approximately fourfold to a value of 6–10%. As with the steady-state results, the SL wye geometry reduces total device DF by a factor of approximately 2, except for the 4.9-μm aerosol case, where deposition is consistently above 50%. With cyclic ventilation conditions, the minimum device deposition (7.3%) and maximum ED (80.3%) are observed for the 880-nm aerosol and SL wye T2 conditions. However, this delivery scenario does not represent maximum lung deposition, as a portion of the 880-nm aerosol will likely be exhaled from the lungs.

As indicated in Table 2, the dose exhaled from the wye geometry (circuit exhaled dose) decreased by a factor of 4 when T2 delivery was used compared with T1. The reason for this reduction is illustrated in Figure 7, which depicts locations of airborne particles at the end of inspiration for T1 and T2 delivery. With T1, a large fraction of particles is suspended in the ventilation system at the end of inhalation and subsequently exhaled through the expiratory line. In contrast, with the T2 delivery, a majority of the aerosol has passed out of the ETT and only a small residual is left airborne. Approximately one half of the inhalation cycle appears adequate to clear a majority of the aerosol from the SL wye and ETT system, which reduces circuit exhaled dose to approximately 10% and below.

Predictions of lung deposition

Predictions of lung deposition based on the Monte Carlo whole-lung model and polydisperse aerosol distributions are reported in Table 3 for cyclic ventilation conditions. Initial delivery conditions in terms of aerosol particle size

Table 2. CFD Predictions of Performance During Cyclic Breathing

Aerosols	$DF_{inlet+wye}$	DF_{ETT}	DF_{device}	*ED*	*Circuit exhaled dose*[a]
CM wye T1					
MMAD = 880 nm	22.4	3.2	25.6	42.3	32.1
MMAD = 1.78 μm	23.1	10.3	33.4	34.4	32.2
MMAD = 4.9 μm	29.7	32.0	61.7	10.3	28.0
CM wye T2					
MMAD = 880 nm	10.3	5.2	15.5	77.4	7.1
MMAD = 1.78 μm	10.3	17.3	27.6	65.9	6.5
MMAD = 4.9 μm	16.0	56.5	72.5	19.9	7.6
SL wye T1					
MMAD = 880 nm	5.8	2.4	8.2	54.5	37.3
MMAD = 1.78 μm	7.9	6.9	14.8	48.0	37.2
MMAD = 4.9 μm	17.3	36.4	53.7	18.3	28.0
SL wye T2					
MMAD = 880 nm	3.7	3.6	7.3	80.3	12.4
MMAD = 1.78 μm	5.7	11.2	16.9	72.2	10.9
MMAD = 4.9 μm	15.1	55.6	70.7	26.0	3.3

The table presents CFD predictions of performance during cyclic breathing including deposition fractions (DFs) in the 10-cm tubing inlet + wye, ETT, and total device, emitted dose (ED) from the ETT, and exhaled dose lost from the ventilation circuit during expiration.

[a]Fraction of dose (as %) lost from the delivery circuit during the exhalation phase of cyclic breathing. This fraction does not include the fraction of dose lost from the lung during exhalation, which is calculated in Table 3.

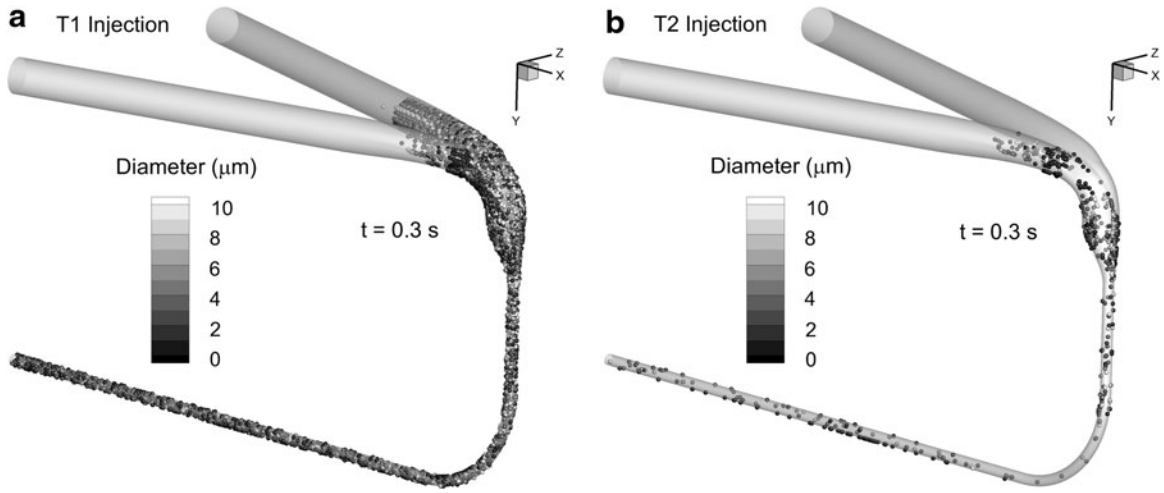

FIG. 7. Positions of airborne particles at the end of the inspiratory phase for the SL wye geometry and MMAD = 1.78-μm aerosol with **(a)** T1 and **(b)** T2 injection strategies.

distribution and timing of the aerosol exiting the ETT were determined from the CFD simulations. The calculated MMADs of the aerosol exiting the ETT and entering the trachea are also reported in Table 3. As an example, aerosol deposition in the CM wye design with T1 and T2 delivery reduced the 4.9-μm aerosol to an MMAD of 1.5 μm. For comparison, the 4.9-μm aerosol when passed through the SL geometry was reduced to approximately 2.0 μm. As for lung DFs and lung exhaled dose, the values reported in Table 3 are in terms of initial dose delivered at the circuit inlet. Therefore, the lung DFs (TB and alveolar) plus the lung exhaled dose equal the ED from the ETT reported in Table 2. For total lung DF, maximum values occur at the intermediate 1.78-μm polydisperse aerosol in all cases, due to high lung exhaled doses for the smallest aerosol particle size and ventilation system depositional losses for the 4.9-μm aerosol (Table 3). The SL design increases the maximum polydisperse lung DF by a factor of 1.2–1.4. Aerosol delivery timing has an even larger effect with T2 delivery increasing DF_{lung} by twofold compared with T1. Maximum TB and lung DFs are 28% and 45.2%, respectively, which are achieved with SL wye T2 and the 1.78-μm aerosol. However, maximum alveolar DF (20%) is achieved with the 880-nm aerosol and SL wye T2 conditions.

Plots of lung deposition for a range of monodisperse aerosol particle sizes are provided in Figure 8 based on the whole-lung model predictions. As with the polydisperse aerosols, both T2 delivery and the SL design are shown to increase DF in all regions considered (lung, TB, and alveolar). For a monodisperse aerosol and cyclic inhalation with the SL

Table 3. Model Predictions of Lung Delivery During Cyclic Breathing

Aerosols	*MMAD lung inlet (μm)*	DF_{TB}[a]	$DF_{alveolar}$[a]	DF_{lung}[a]	*Lung exhaled dose*[b]
CM wye T1					
MMAD = 880 nm	0.70	8.7	9.0	17.8	24.5
MMAD = 1.78 μm	1.23	12.5	7.3	19.7	14.7
MMAD = 4.9 μm	1.46	4.6	2.2	6.8	3.5
CM wye T2					
MMAD = 880 nm	0.70	15.6	17.3	32.9	44.5
MMAD = 1.78 μm	1.24	24.1	14.1	38.2	27.7
MMAD = 4.9 μm	1.53	9.2	4.3	13.5	6.4
SL wye T1					
MMAD = 880 nm	0.70	10.8	11.3	22.1	32.4
MMAD = 1.78 μm	1.28	18.3	9.5	27.8	20.2
MMAD = 4.9 μm	2.00	10.1	3.3	13.3	5.0
SL wye T2					
MMAD = 880 nm	0.70	16.4	20.0	36.4	43.9
MMAD = 1.78 μm	1.28	28.0	17.2	45.2	27.0
MMAD = 4.9 μm	1.90	13.9	5.7	19.6	6.4

The table presents model predictions of lung delivery during cyclic breathing, including the MMAD of the polydisperse aerosol entering the lungs, deposition fraction (DF) in the TB, alveolar, and total lung, as well as exhaled dose exiting the lungs.

[a]All DFs are in terms of initial dose injected at the delivery circuit inlet and therefore take into account losses in the delivery system (wye and ETT).

[b]Percentage of aerosol that enters the lungs and is then exhaled back into the delivery system and out the expiratory line.

wye and T2 delivery, total lung DF near 60% can be achieved with a 2.5-μm aerosol. Maximum TB and alveolar DFs of 43% and 21% can be achieved with 2.8-μm and 1.9-μm size aerosols. These values take into account depositional losses in the delivery circuit, reasonable tidal volume for an infant (25 mL), cyclic inhalation, and exhaled dose fractions.

Discussion

In this study, a new combination of *in vitro* experiments, CFD simulations, and whole-lung modeling was implemented to assess the optimal delivery of aerosols to the lungs of a newborn infant on mechanical ventilation. The approach leverages the strengths of each method in order to predict the transport and deposition of aerosols through the delivery system and into the lungs under cyclic ventilation conditions. *In vitro* experiments of aerosol delivery typically consider steady-state or cyclic conditions and assume that the particles or droplets exiting the ETT deposit in the lungs. This approach neglects the exhaled fraction of the aerosol such that aerosol size optimization is not possible. Calculation of the expired dose during mechanical ventilation delivery previously required either human subject experiments, which are challenging to perform with infants, or animal model studies. In contrast, the CFD approach implemented in this study captures deposition within the ventilation circuit, as well as lung deposition and exhaled dose. As demonstrated in Tables 2 and 3, combinations of ventilator circuit and lung exhaled doses were as high as 70% for the 880-nm aerosol. Even for the 4.9-μm aerosol, total exhaled dose was 35% in the infant lung model. By considering both deposition and exhaled dose, the new approach used in this study can approximate optimal delivery conditions for depositing aerosols in the lungs of infants. In the current study, optimal delivery conditions were evaluated in terms of aerosol particle size (for polydisperse distributions and monodisperse particles), design of the wye component, and aerosol delivery timing.

With regard to the selection of an aerosol particle size for maximum delivery efficiency of medications to infants, both *in vitro* and CFD predictions indicated an increase in ED from the ETT as aerosol particle size decreased, which was expected. However, it was surprising how well the smaller aerosol particle sizes penetrated the ventilation circuit and were available to enter the lungs. With the small and intermediate aerosols, steady-state predictions of ED from the ETT were in the range of 80–90% for the CM and SL wye systems. In contrast, delivery of the more conventional 4.9-μm size resulted in steady-state ED values of approximately 10%. The effect of aerosol particle size is best illustrated in Figure 6b, where both wye devices have total DFs below 20% for monodisperse aerosols less than 2 μm. Increasing the aerosol particle size to the conventional range of 4–7 μm results in a dramatic increase in total ventilation circuit DF. The ED from the ETT was significantly reduced with cyclic inhalation conditions due to high exhaled dose from the circuit (Table 2). However, circuit exhaled dose is not largely affected by particle size. Fortunately, the small and intermediate size aerosols were found to deposit efficiently in the TB and alveolar airways of an infant (Table 3). For the polydisperse distributions, an optimal total lung deposition efficiency of 45.2% was achieved with the 1.78-μm aerosol, SL wye, and T2 delivery (Table 3). With this configuration, the smallest aerosol (880 nm) had a high total exhaled dose (56.3%), but also the highest alveolar delivery efficiency with a value of 20%. Considering monodisperse

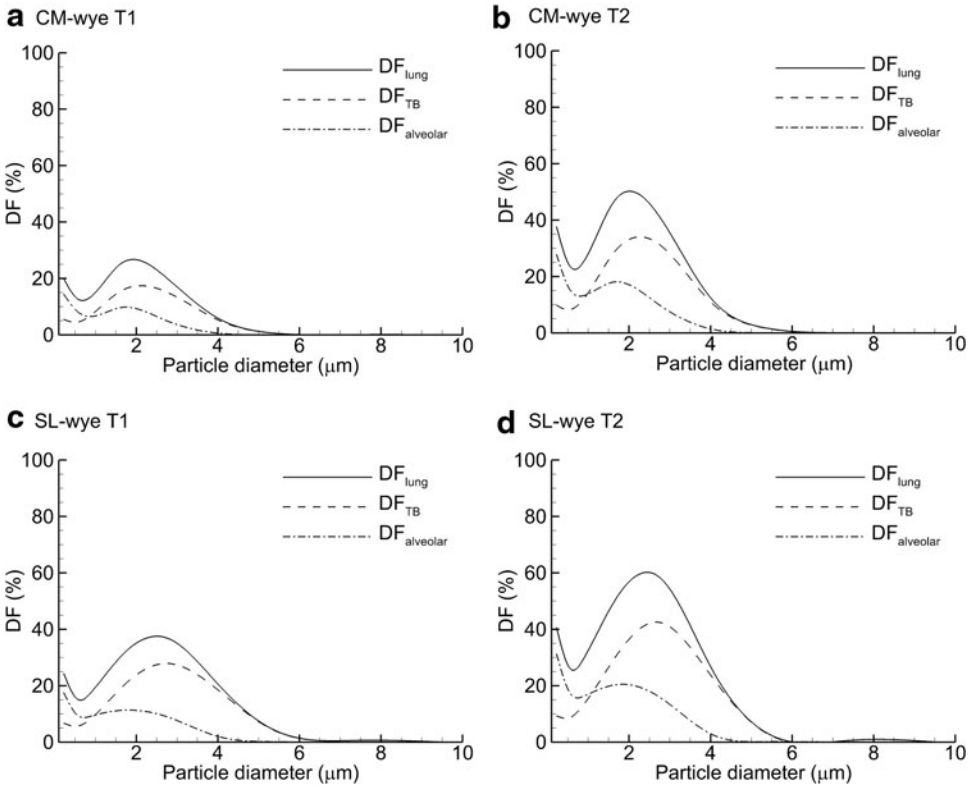

FIG. 8. Predictions of DF in the total lung, TB, and alveolar regions for monodisperse aerosols and the following delivery device and injection scenarios: **(a)** CM wye and T1, **(b)** CM wye and T2, **(c)** SL wye and T1, and **(d)** SL wye and T2.

aerosols allowed for the selection of optimal particle sizes with a maximum lung DF value of 60% for a 2.5-μm aerosol, and a size range of 1.9–2.8 μm for maximizing aerosol deposition in the alveolar and TB regions.

The SL wye geometry played an important role in achieving the high lung delivery efficiencies reported in this study. Compared with the CM wye system, the SL design typically reduced deposition in the wye by two- to fourfold, but reductions as large as sevenfold were also observed. As delivery through the wye improves, depositional loss in the ETT also increases, which limits the overall performance of the delivery system. However, total device deposition was typically reduced by a factor of 2 with the SL system for the small and intermediate particle sizes. With the 4.9-μm aerosol, DFs were typically above 50% for both wye connectors, but the SL design still reduced depositional losses. Another benefit of the SL wye concept was the size distribution of the aerosol exiting the ETT. Based on CFD simulations, polydisperse aerosols exiting the ETT and entering the lungs were either larger or the same size with the SL wye design compared with the CM wye. Larger aerosols entering the lungs are expected to deposit and be retained at a higher rate than smaller particles.

Timing of the aerosol delivery is an important issue, with current studies reporting mixed results in terms of lung delivery and deposition.[11,17,29] Due to very low tidal volumes, aerosol synchronization effects are strongly influenced by the position of the nebulizer within the ventilation line. In this study, a CFD approximation of synchronization was used with the aerosol either delivered during inhalation (T1) or only delivered over the first half of the inhalation waveform (T2). Previous studies have not considered timing the delivery over a portion of the inspiratory cycle during invasive mechanical ventilation. Based on the low tidal volume used, it is important for the aerosol to clear the ventilator circuit and be moved into the lungs before exhalation occurs. With synchronized T1 delivery, approximately 30–40% of the aerosol remains in the ventilator circuit and is then exhaled. In contrast, delivering the aerosol with T2 delivery decreases the ventilator exhaled dose by a factor of 4 and increases lung deposition of the aerosol by a factor of 2. Therefore, delivering the aerosol over only a portion of the inspiratory flow appears to be an important strategy for improving respiratory drug delivery to infants on mechanical ventilation. Successful implementation of this approach requires that the aerosol be delivered close to the wye so that the ventilation system can be cleared of aerosol during the inspiratory cycle.

This study seeks to maximize delivery efficiency and defines optimal delivery as the approach that provides the lowest aerosol loss and highest lung deposition relative to the nominal dose at the inlet of the circuit. However, it is critically important to also consider the mass of drug that each technique delivers to the lungs. It is known that different size particles deliver different masses of drug when deposited. For example, a single dry AS particle with a 4.9-μm diameter will deliver approximately 173 times more drug mass than a single 880-nm dry particle. However, in this study, both the 4.9-μm and 880-nm aerosols were formed using the same nebulizer and same initial AS solution concentration. The 4.9-μm aerosol was delivered as droplets, and the 880-nm aerosol was formed by passage through the mixer-heater and delivered as dry particles. Therefore, the maximum and minimum aerosol sizes considered provided approximately the same nebulized dose. In this study, the reduced nominal dose associated with the smallest aerosol was due to the experimental setup where the 880-nm aerosol stream exiting the mixer-heater was split to create a 5 L/min flow rate, whereas splitting was not needed for the 4.9-μm aerosol. A future version of the small aerosol generator will allow for the direct delivery of 5 L/min flow, eliminating the need for splitting the aerosol stream and providing equal nominal doses for both the small 880-nm and conventional 4.9-μm aerosols. With these equal nominal doses, the use of the SL wye and T2 delivery then provides 5 times more drug mass to the lungs compared with the CM wye, T1 delivery, and the conventional 4.9-μm aerosol based on improved efficiency (Table 3). This significant increase in lung dose should be taken into consideration and the administered dose adjusted accordingly for implementation of the optimized system in human subjects.

Drug mass deposited in the lungs should also be considered for T1 versus T2 delivery. Injecting the aerosol over the first half of the inspiratory cycle was found to be 2 times more efficient in terms of lung deposition; however, this approach only delivers one half the nebulized dose in a set amount of time. Therefore, although T1 delivery wastes a larger fraction of the nebulized dose, lung deposition of drug mass is equal between T1 and T2 delivery. As a result, T1 and T2 approaches may be equally acceptable for medications with mild side effects, wide therapeutic windows, and low cost. However, for more advanced respiratory medications, it becomes important to minimize loss and have better knowledge of the lung deposited dose. Furthermore, it is expected that variability in lung delivered dose increases with increasing depositional loss in the ventilator circuit. Therefore, T2 delivery may be preferred for many aerosolized medications as a means to reduce drug waste, better control the lung delivered dose, and reduce variability associated with different mechanical ventilation circuits.

In delivering aerosols to ventilated infants, it is critical to consider the tidal volume, dead space in the ventilation circuit, and airway volume. In the current study of a 3.6-kg infant, the tidal volume was 25 cm^3, dead space between aerosol delivery and the end of the ETT was 5.7 cm^3, and airway volume through B15 (TB airways) was 16.7 cm^3. Based on mean flow rates in each component, the aerosol should only reach the upper part of the alveolar airways. However, nonuniform velocity profiles and flow through the bifurcation structure enhance aerosol transport and increase delivery to the lower airways.[50] As a result, sufficient alveolar deposition is realized with the current delivery approach. Delivery efficiency to the lower lung will significantly decrease for smaller infants using the same system. For example, a preterm 1.5-kg neonate has a tidal volume of approximately 9 mL.[34] In this case, once the aerosol is past the ETT (6.7 cm^3), there is only 2.3 mL of volume to move the aerosol through the lungs. Assuming the Phalen *et al.*[23] lung correlations apply to preterm infants, the aerosol would only reach approximately B10 and would likely not reach the alveolar airways. Delivery efficiency to the entire lung could be improved in this case with an SL wye geometry that further reduces ventilation dead space.

Results of the current study for conventional-sized aerosols and the CM wye are in general agreement with previous

in vitro and *in vivo* studies. For example, Dubus *et al*.[11] employed a 3-mm ETT in a ventilated infant model using macaques with an average weight of 2.6 kg. The Aeroneb Pro nebulizer was used in synchronized and continuous modes producing MMADs of 2.8 and 4.6 μm, respectively. The resulting lung delivery efficiencies were 12.6–14%, with no statistical difference between the two modes of ventilation. In comparison, the conventional aerosol particle size of 4.9 μm used in this study resulted in lung DFs of 6.8–13.5%. Differences in deposition may be due to the larger tidal volume and higher flow rates used in the current study, which reduced exhaled dose compared with that of Dubus *et al*.[11]

Limitations of the current study include evaluation of delivery to a single average full-term infant with one set of ventilation conditions, the need to interface model results between the ETT and lung, a lack of wall motion in the alveolar region, and a need to further validate the numerical *in vivo* predictions. Aerosol delivery to infants is highly variable and depends heavily on ventilator settings, disease state, and lung volume. Additional studies are needed to determine optimal delivery conditions across a range of ventilator settings and patient variables. The approach selected in this study interfaces validated CFD predictions with a whole-lung model of aerosol deposition. There may be some information lost at this interface, such as deposition in the ventilator circuit of aerosols exhaled from the lung. However, this fraction does not influence the lung deposition estimates. Finally, whole-lung one-dimensional models have a number of known limitations. In the current model, propagation of the aerosol through the airways was based on mean velocities and the alveolar walls did not move. Both of these assumptions are expected to provide conservatively low estimates of alveolar deposition. Furthermore, comparisons of the whole-lung model predictions are needed with *in vivo* data of infants receiving mechanical ventilation. The current model is based on a long history of well developed whole-lung deposition approximations.[47–49,51] Nevertheless, until further validation with *in vivo* data is performed, the current results may best serve to compare expected delivery rates based on the factors of wye component selection, delivery timing, and aerosol particle size.

Conclusions

In conclusion, optimal delivery conditions can significantly increase the deposition of aerosol in the lungs of infants receiving mechanical ventilation compared with the current standard of care. The delivery of aerosols smaller than those typically delivered to adults significantly improved transport through the ventilation system, with depositional losses lower than 10% for some cases. Due to small airway sizes, small (880 nm) and intermediate (1.78 μm) aerosols are then effectively retained in the infant lungs. Implementation of an SL wye design reduced depositional losses in the wye by a factor of approximately 2–4 and improved lung delivery efficiency by a factor of approximately 2 compared with a CM device. Delivery of the aerosol over the first half of the inspiratory cycle reduced exhaled dose from the ventilation circuit by a factor of 4. Optimal lung delivery was achieved with an SL wye configuration and T2 delivery of the aerosol. Maximum lung deposition of approximately 50% was achieved with a realistic polydisperse aerosol produced with a custom mixer-heater and having an MMAD of 1.78 μm. An analysis of idealized monodisperse aerosol particle sizes indicted that optimal lung, TB, and alveolar delivery could be achieved with an aerosol particle size range of 1.9–2.8 μm. The new approach used in this study appears to be an effective way to predict both depositional losses in the delivery circuit and lung deposition prior to costly and difficult to perform human subjects or animal model testing. Future studies are needed to evaluate a broader set of pediatric patients, include a range of ventilation conditions, develop a method for controlled aerosol delivery during a portion of the inspiration phase, generate the new target aerosol particle sizes at low flow rates, and test delivery *in vivo*.

Acknowledgments

Research reported in this publication was supported by the Eunice Kennedy Shriver National Institute of Child Health and Human Development of the National Institutes of Health under Award Number R21HD073728. The content is solely the responsibility of the authors and does not necessarily represent the official views of the National Institutes of Health.

Author Disclosure Statement

The authors declare that there are no conflicts of interest.

References

1. Dhand R: Inhalation therapy in invasive and noninvasive mechanical ventilation. Curr Opin Crit Care. 2007;13:27–38.
2. Dhand R: Aerosol delivery during mechanical ventilation: from basic techniques to new devices. J Aerosol Med Pulm Drug Deliv. 2008;21:45–60.
3. Cole CH, Colton T, Shah BL, Abbasi S, MacKinnon BL, Demissie S, and Frantz ID: Early inhaled glucocorticoid therapy to prevent bronchopulmonary dysplasia. N Engl J Med. 1999;340:1005–1010.
4. Sood BG, Delaney-Black V, Aranda JV, and Shankaran S: Aerosolized PGE_1: a selective pulmonary vasodilator in neonatal hypoxemic respiratory failure results of a phase I/II open label clinical. Pediatr Res. 2004;56:579–585.
5. Armangil D, Yurdakok M, Korkmaz A, Yigit S, and Tekinalp G: Inhaled beta-2 agonist salbutamol for the treatment of transient tachypnea of the newborn. J Pediatr. 2011;159:398–403.
6. Shah V, Ohlsson A, Halliday HL, and Dunn MS: Early administration of inhaled corticosteroids for preventing chronic lung disease in ventilated very low birth weight preterm neonates. Cochrane Database Syst Rev. 2007;(4):CD002057.
7. Berggren E, Liljedahl M, Winbladh B, Andreasson B, Cursted T, and Robertson B: Pilot study of nebulized surfactant therapy for neonatal respiratory distress syndrome. Acta Paediatr. 2000;89:460–464.
8. Fink JB: Aerosol delivery to ventilated infant and pediatric patients. Respir Care. 2004;49:653–665.
9. Mazela J, and Polin RA: Aerosol delivery to ventilated newborn infants: historical challenges and new directions. Eur J Pediatr. 2011;170:433–444.
10. Rubin BK, and Fink JB: Aerosol therapy for children. Respir Care Clin N Am. 2001;7:175–213.

11. Dubus JC, Vecellio L, De Monte M, Fink JB, Grimbert D, Montharu J, Valat C, Behan N, and Diot P: Aerosol deposition in neonatal ventilation. Pediatr Res. 2005;58:10–14.
12. Mazela J, Chmura K, Kulza M, Henderson C, Gregory TJ, Moskal A, Sosnowski TR, Florek E, Kramer L, and Keszler M: Aerosolized albuterol sulfate delivery under neonatal ventilatory conditions: *in vitro* evaluation of a novel ventilator circuit patient interface connector. J Aerosol Med Pulm Drug Deliv. 2013 [Epub ahead of print].
13. Everard ML, Stammers J, Hardy JG, and Milner AD: New aerosol delivery system for neonatal ventilator circuits. Arch Dis Child. 1992;67:826–830.
14. Garner SS, Southgate M, Wiest DB, Brandeburg S, and Annibale DJ: Albuterol delivery with conventional and synchronous ventilation in a neonatal lung model. Pediatr Crit Care Med. 2002;3:52–56.
15. Fok TF, Al-Essa M, Monkman S, Dolovich M, Girard L, Coates G, and Kirpalani H: Pulmonary deposition of salbutamol aerosol delivered by metered dose inhaler, jet nebulizer, and ultrasonic nebulizer in mechanically ventilated rabbits. Pediatr Res. 1997;42:721–727.
16. Fok TF, Monkman S, Dolovich M, Gray S, Coates G, Paes B, Rashid F, Newhouse M, and Kirpalani H: Efficiency of aerosol medication delivery from a metered dose inhaler versus jet nebulizer in infants with bronchopulmonary dysplasia. Pediatr Pulmonol. 1996;21:301–309.
17. Sidler-Moix AL, Dolci U, Berger-Gryllaki M, Pannatier A, Cotting J, and Di Paolo ER: Albuterol delivery in an in vitro pediatric ventilator lung model: comparison of jet, ultrasonic, and mesh nebulizers. Pediatr Crit Care Med. 2013;14: E98–E102.
18. Ari A, Atalay OT, Harwood R, Sheard MM, Aljamhan EA, and Fink JB: Influence of nebulizer type, position, and bias flow on aerosol drug delivery in simulated pediatric and adult lung models during mechanical ventilation. Respir Care. 2010;55:845–851.
19. Ahrens RC, Ries RA, Popendorf W, and Wiese JA: The delivery of therapeutic aerosols through endotracheal-tubes. Pediatr Pulmonol. 1986;2:19–26.
20. Heyder J, Gebhart J, Rudolf G, Schiller CF, and Stahlhofen W: Deposition of particles in the human respiratory tract in the size range of 0.005–15 microns. J Aerosol Sci. 1986;17: 811–825.
21. Stahlhofen W, Rudolf G, and James AC: Intercomparison of experimental regional aerosol deposition data. J Aerosol Med. 1989;2:285–308.
22. Kim CS, and Jaques PA: Respiratory dose of inhaled ultrafine particles in healthy adults. Philos Trans R Soc Lond A Math Phys Eng Sci. 2000;358:2693–2705.
23. Phalen RF, Oldham MJ, Beaucage CB, Crocker TT, and Mortensen JD: Postnatal enlargement of human tracheobronchial airways and implications for particle deposition. Anat Rec. 1985;212:368–380.
24. Hofmann W, Martonen TB, and Graham RC: Predicted deposition of nonhygroscopic aerosols in the human lung as a function of subject age. J Aerosol Med. 1989;2: 49–67.
25. Asgharian B, Menache MG, and Miller FJ: Modeling age-related particle deposition in humans. J Aerosol Med. 2004; 17:213–224.
26. Ivri E, and Fink J: Aerosol delivery apparatus and method for pressure-assisted breathing systems. United States Patent. 2007; No. 7,290,541 B2. Available at www.google.com .bz/patents/US7290541. Accessed November 4, 2013.
27. Longest PW, Golshahi L, and Hindle M: Improving pharmaceutical aerosol delivery during noninvasive ventilation: effects of streamlined components. Ann Biomed Eng. 2013;41: 1217–1232.
28. Miller DD, Amin MM, Palmer LB, Shah AR, and Smaldone GC: Aerosol delivery and modern mechanical ventilation—*in vitro/in vivo* evaluation. Am J Respir Crit Care Med. 2003; 168:1205–1209.
29. Turpeinen M, and Nikander K: Nebulization of a suspension of budesonide and a solution of terbutaline into a neonatal ventilator circuit. Respir Care. 2001;46:43–48.
30. Longest PW, Spence BM, Holbrook LT, Mossi KM, Son Y-J, and Hindle M: Production of inhalable submicrometer aerosols from conventional mesh nebulizers for improved respiratory drug delivery. J Aerosol Sci. 2012;51:66–80.
31. Longest PW, Walenga RL, Son Y-J, and Hindle M: High-efficiency generation and delivery of aerosols through nasal cannula during noninvasive ventilation. J Aerosol Med Pulm Drug Deliv. 2013;26:266–279.
32. National Centers for Health Statistics: Length-for-age and weight for age percentiles. 2000. Available at www.cdc.gov/growthcharts. Accessed November 4, 2013.
33. Dunnill MS: Postnatal growth of the lung. Thorax. 1962;17: 329–333.
34. Walsh BK, and DiBlasi RM: Mechanical ventilation of the neonate and pediatric patient. In: BK Walsh, MP Czervinske, and RM DiBlasi, (eds). *Perinatal and Pediatric Respiratory Care*. Saunders Elsevier, St. Louis, MO; pp. 325–347, 2010.
35. Longest PW, and Hindle M: Evaluation of the Respimat Soft Mist inhaler using a concurrent CFD and *in vitro* approach. J Aerosol Med Pulm Drug Deliv. 2009;22:99–112.
36. Xi J, Longest PW, and Martonen TB: Effects of the laryngeal jet on nano- and microparticle transport and deposition in an approximate model of the upper tracheobronchial airways. J Appl Physiol. 2008;104:1761–1777.
37. Longest PW, and Vinchurkar S: Validating CFD predictions of respiratory aerosol deposition: effects of upstream transition and turbulence. J Biomech. 2007;40:305–316.
38. Longest PW, Hindle M, Das Choudhuri S, and Xi J: Comparison of ambient and spray aerosol deposition in a standard induction port and more realistic mouth–throat geometry. J Aerosol Sci. 2008;39:572–591.
39. Vinchurkar S, and Longest PW: Evaluation of hexahedral, prismatic and hybrid mesh styles for simulating respiratory aerosol dynamics. *Comput Fluids*. 2008;37:317–331.
40. Longest PW, and Vinchurkar S: Effects of mesh style and grid convergence on particle deposition in bifurcating airway models with comparisons to experimental data. Med Eng Phys. 2007;29:350–366.
41. Longest PW, Hindle M, Das Choudhuri S, and Byron PR: Numerical simulations of capillary aerosol generation: CFD model development and comparisons with experimental data. Aerosol Sci Technol. 2007;41:952–973.
42. Longest PW, Kleinstreuer C, and Buchanan JR: Efficient computation of micro-particle dynamics including wall effects. *Comput Fluids*. 2004;33:577–601.
43. Longest PW, and Xi J: Effectiveness of direct Lagrangian tracking models for simulating nanoparticle deposition in the upper airways. Aerosol Sci Technol. 2007;41:380–397.
44. Longest PW, and Hindle M: Numerical model to characterize the size increase of combination drug and hygroscopic excipient nanoparticle aerosols. Aerosol Sci Technol. 2011;45: 884–899.

45. Longest PW, and Hindle M: Condensational growth of combination drug-excipient submicrometer particles: comparison of CFD predictions with experimental results. Pharm Res. 2012;29:707–721.
46. Hindle M, and Longest PW: Condensational growth of combination drug-excipient submicrometer particles for targeted high efficiency pulmonary delivery: evaluation of formulation and delivery device. J Pharm Pharmacol. 2012;64: 1254–1263.
47. Koblinger L, and Hofmann W: Monte Carlo modeling of aerosol deposition in human lungs. Part I: Simulation of particle transport in a stochastic lung structure. J Aerosol Sci. 1990;21:661–674.
48. Koblinger L, and Hofmann W: Analysis of human lung morphometric data for stochastic aerosol deposition calculations. Phys Med Biol. 1985;30:541–556.
49. Asgharian B, Hofmann W, and Bergmann R: Particle deposition in a multiple-path model of the human lung. Aerosol Sci Technol. 2001;34:332–339.
50. Park SS, and Wexler AS: Particle deposition in the pulmonary region of the human lung: a semi-empirical model of single breath transport and deposition. J Aerosol Sci. 2007; 38:228–245.
51. Asgharian B, and Anjilvel S: A Monte Carlo calculation of the deposition efficiency of inhaled particles in lower airways. J Aerosol Sci. 1994;25:711–721.

Received on July 9, 2013
in final form, October 17, 2013

Reviewed by:
Chong Kim
Graham Johnson

Address correspondence to:
Dr. P. Worth Longest
Virginia Commonwealth University
401 West Main Street
P.O. Box 843015
Richmond, VA 23284-3015

Email: pwlongest@vcu.edu